SOILS AND FOUNDATIONS Vol. 47, No. 4, 783–797, Aug. 2007
Japanese Geotechnical Society

SEISMIC BEARING CAPACITY OF A CIRCULAR FOOTING ON A HETEROGENEOUS COHESIVE SOIL

CHARISIS THEODOROU CHATZIGOGOS[i], ALAIN PECKER[i] and JEAN SALENÇON[i]

ABSTRACT

This study concerns the determination of the seismic bearing capacity of a circular footing resting on a purely cohesive heterogeneous soil layer. The problem is treated using the kinematic approach of the Yield Design theory. The soil strength is modelled by the Tresca criterion with C_0 the cohesion at the soil surface and G the vertical cohesion gradient. The loading process of the system is described by four loading parameters: an inclined force (N: vertical component, V: horizontal component), a moment (M) acting at the center of the footing and horizontal uniform inertial forces (F_h) acting in the soil volume during the seismic excitation. Two cases are considered for the soil: a soil with an infinite tensile strength and a soil with zero tensile strength. The soil-footing interface is considered purely cohesive with zero tensile strength. The study presents optimal upper bounds for the ultimate combinations of the dimensionless loading parameters (N, V, M, F_h) by the examination of a series of three-dimensional virtual kinematic mechanisms of failure. The results are presented in the form of surfaces in the space of the parameters (N, V, M) for a range of values of F_h.

Key words: bearing capacity, circular footings, cohesive soils, earthquake resistant, shallow foundation (**IGC**: E3/HI)

INTRODUCTION

The motivation for the study of the seismic bearing capacity of shallow foundations has been given by a series of field observations after several major earthquakes within the last twenty five years, which revealed a particular type of foundation failure without the presence of liquefaction in the supporting soil layers. The main characteristics of this failure mechanism are: a) large permanent rotations at the foundation level (sometimes leading to the toppling of the structure) without significant structural damage in the superstructure (c.f., Fig. 1), b) creation of a zone of detachment at the soil-foundation interface (c.f., Fig. 2), c) development of a failure mechanism within the soil volume and d) large vertical displacements (often of the order of 1 m) (c.f., Fig. 3). Such cases of foundation failure have been reported mainly after the 1985 Guerrero-Michoacán earthquake (Mendoza and Auvinet, 1988), and also after more recent earthquakes (e.g., 1990 Luzon earthquake; 1999 Koçaeli earthquake, etc.). The same failure mechanism was also identified experimentally: Zeng and Steedman (1998), by performing a series of centrifuge tests at the University of Cambridge (UK), were able to reproduce the main characteristics of this failure mechanism and to underline the particularly negative effect of high vertical load intensity and eccentricity; similarly Knappett et al. (2006), by means of shaking table tests performed at the University of Cambridge (UK) and with the aid of the Particle Image Velocimetry technique measured the velocity field at failure within the soil volume and studied the effect of the intensity and frequency content of the seismic action together with the influence of the depth of embedment of the foundation. It was thus understood that a shallow foundation may experience a bearing capacity failure during an earthquake excitation due to the combined negative effect of a highly eccentric and inclined load on the foundation originating

Fig. 1. Large permanent rotations at the foundation level of a building after the 1999 Koçaeli earthquake (*Source: http://nisee.berkeley.edu/elibrary*)

[i] Laboratory of Solid Mechanics CNRS UMR 7649, Department of Mechanics, Ecole Polytechnique, France (alain.pecker@geodynamique.com).
The manuscript for this paper was received for review on October 16, 2006; approved on April 4, 2007.
Written discussions on this paper should be submitted before March 1, 2008 to the Japanese Geotechnical Society, 4-38-2, Sengoku, Bunkyo-ku, Tokyo 112-0011, Japan. Upon request the closing date may be extended one month.

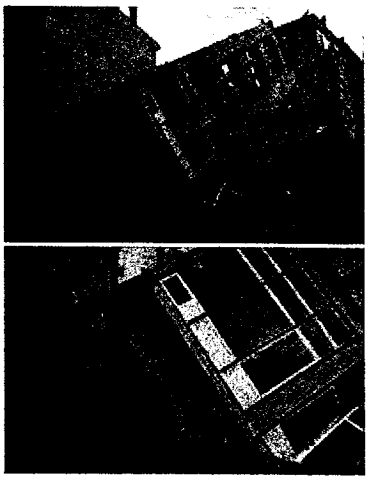

Fig. 2. Creation of a zone of detachment at the soil-foundation interface. The building has completely toppled. 1999 Koçaeli earthquake (*Source: http://nisee.berkeley.edu/elibrary*)

Fig. 3. Development of a mechanism of failure within the soil volume accompanied by significant vertical displacements. Building in Mexico City after the 1985 Guerrero-Michoacán earthquake

from the inertial response of the superstructure and of the action of the inertial body forces within the soil volume. This can occur even without a decrease in the soil strength from liquefaction or other related soil softening phenomena.

From a theoretical point of view, numerous studies have been published on the subject. One initial approach to the problem of seismic bearing capacity was to work within the classical framework of Terzaghi's bearing capacity formula. This was achieved by modifying the bearing capacity factors N_c, N_q, N_γ in order to account for the effect of the inertial body forces in the soil volume during the seismic excitation, while applying appropriate correction factors for the load eccentricity and inclination. Following this idea, Sarma and Iossifelis (1990), Richards et al. (1993) and more recently Fishman et al. (2003) conducted limit equilibrium analyses whereas Kumar and Rao (2002) worked with the slip line method (without constructing however, a complete stress field) and suggested bearing capacity factors N_c, N_q, N_γ as functions of a characteristic seismic horizontal acceleration. A second approach was developed in parallel, as a more convenient way to visualize the effects of overturning moments and horizontal forces on the footing. It is based on the representation of the seismic bearing capacity of the foundation system by an "ultimate surface" (surface of ultimate combinations of loads) in the space of the loading parameters (N: vertical force, V: horizontal force, M: overturning moment) which would vary as a function of the intensity of the horizontal inertial forces F_h in the soil volume. Following this idea, Pecker and Salençon (1991) established upper bounds of the exact ultimate combinations of N, V, M and F_h for a strip footing on a homogeneous purely cohesive soil whereas Salençon and Pecker (1995a, b) provided very close lower and upper bounds of the ultimate combinations of N, V and M for the same foundation configuration. Paolucci and Pecker (1997a) extended the upper bound solutions to the case of rectangular footings on purely cohesive soils and Dormieux and Pecker (1995) and Paolucci and Pecker (1997b) to the case of strip footings on homogeneous purely frictional soils (including the effects of the unit weight of the soil and the vertical earthquake acceleration). All these results were incorporated in the European norms for earthquake resistant design of civil structures (Eurocode 8-Part 5: prEN 1998-5) and were numerically "fitted" by an analytical expression defining the seismic bearing capacity of a strip footing on either a purely cohesive or a purely frictional homogeneous soil (Pecker, 1997). This analytical expression represents the ultimate loads supported by the footing as a surface in the (N, V, M) space and is function of the soil strength criterion and the values of the other loading parameters of the system (horizontal and vertical seismic acceleration and soil unit weight). The Eurocode 8 expression for the seismic bearing capacity of shallow foundations, though unifying and reflecting a large volume of results, has its limitations: it can only be applied to strip footings on homogeneous soils, either purely cohesive or purely frictional.

The present study aims at extending the existing theoretical results for the seismic bearing capacity of shallow foundations to the case of a circular footing resting on the surface of a heterogeneous purely cohesive soil layer. Due to similarities between the problems concerned, a lot of insight can be gained from the many studies relating to the problem of bearing capacity of strip and circular footings subjected to a combined (N, V, M) loading, that have been performed in the context of the offshore industry. Randolph et al. (2005), in a state-of-the-art report, summarized the large variety of solutions, both in terms of the examined configurations and in terms of the implemented methods of analysis, for strip and circular footings of offshore structures. Although these solutions cover a lot of features (combined loading, soil heterogeneity, depth of embedment etc.), they do not incorporate the effect of the seismic inertial forces in the soil volume. Furthermore, they usually make the assumption of perfect adhesion at the soil-footing interface, which is a more realistic assumption for offshore shallow foundations. Thus, they do not allow for the creation of a zone of detachment between the soil and the footing, which is an essential characteristic of seismic bearing capacity

failure of shallow foundations.

The problem is treated herein using the kinematic approach of the Yield Design theory (Salençon, 1983, 1990, 2002), thus providing upper bound estimates of the ultimate seismic loads supported by the soil-foundation system. It must be clear that the question of liquefaction is not addressed in this study: it is considered that the risk of liquefaction at the soil site, where the foundation will be installed, has been addressed at an initial stage, prior to the seismic bearing capacity evaluation.

PROBLEM FORMULATION

The Yield Design theory makes it possible to determine upper bound estimates for the ultimate loads that can be supported by a structure once three pieces of information are available, namely: as regards the structure itself, its geometry and the loading process it is submitted to and, as regards the constituent materials, their strength criteria, whatever the physical phenomena they are related to. Since it does not need incorporating any other data such as the constitutive law of the materials at failure, it should be kept in mind that the obtained results are but upper bound estimates and that no information can be obtained regarding the displacements.

Geometry

The geometry of the considered configuration is described as a circular footing of radius r, resting on the surface of the soil.

Strength Criteria

a. Strength criterion of the soil. The soil is considered as a heterogeneous purely cohesive material. Its strength is described by the Tresca failure criterion; its cohesion c is considered to vary linearly with depth:

$$c = C_0 + Gz, \tag{1}$$

where C_0 is the value of soil cohesion at the soil surface and G is the vertical gradient of the soil cohesion (c.f., Fig. 4). Two separate cases have been considered in order to evaluate the influence of the tensile strength of the soil:

- The classical Tresca criterion described by the equation:

$$f(\underline{\underline{\sigma}}) = |\sigma_1 - \sigma_3| - 2c \leq 0 \tag{2}$$

- The Tresca criterion with zero strength to tension (a zero tension "cut-off") described by the equation:

$$f(\underline{\underline{\sigma}}) = \sup\{|\sigma_1 - \sigma_3| - 2c, \sigma_1\} \leq 0 \tag{3}$$

In Eqs. (2), (3) σ_1 and σ_3 are the major and minor principal stresses of the stress tensor $\underline{\underline{\sigma}}$. Stresses are considered positive in tension. These criteria are depicted in Fig. 5(a) and 5(b) in the (σ, τ) space, where σ and τ denote the normal and tangential stress components respectively, acting on any facet within the soil mass. Anticipating on the concept to be introduced in section 3 from Eqs. (11)-(15), the corresponding relevant velocity vectors are also illustrated in this Figure.

b. Strength criterion of the interface. The soil-footing interface is also considered as purely cohesive and its strength is modelled by the Tresca strength criterion with no tensile strength (zero tension "cut-off"). This choice comes from observing that the occurrence of detachment zones between the footing and the soil is an essential characteristic of seismic bearing capacity failure. The interface cohesion is considered equal to C_0. This criterion, represented in Fig. 6, is described by the equation:

$$f(\sigma, \tau) = \sup\{|\tau| - C_0, \sigma\} \leq 0 \tag{4}$$

Loading Process

The loading of the soil-foundation system is developed during a seismic excitation. The propagation of the seis-

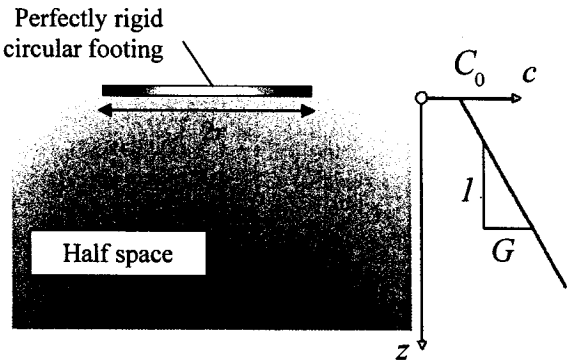

Fig. 4. System geometry and variation of soil cohesion with depth

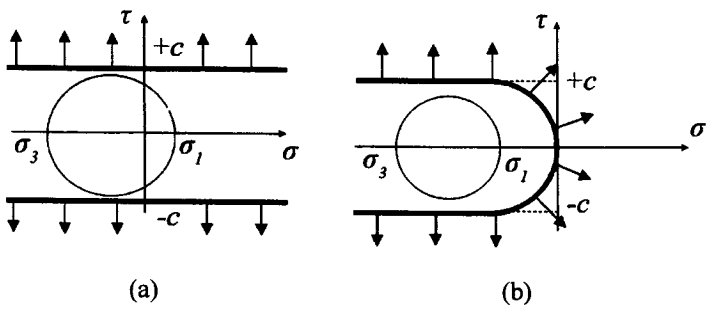

Fig. 5. a) Classical Tresca criterion (with infinite tensile strength) and b) Tresca criterion with no tensile strength (zero tension "cut-off") and corresponding relevant velocity vectors

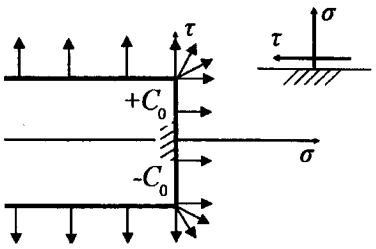

Fig. 6. Tresca criterion without tensile resistance for the soil-footing interface and corresponding relevant velocity vectors

mic waves leads to the inertial response of the soil and of the superstructure through the soil-structure interaction. The hypothesis of a perfectly rigid footing allows for the description of the forces originating from the superstructure and acting on the footing by means of the resultant force and moment acting at a specific reference point of the footing. This reaction is herein described by the following loading parameters: a vertical force $\underline{N}$, a horizontal force $\underline{V}$ and a moment $\underline{M}$ acting at the center of the footing. It is noted that the effect of the forces acting on the footing itself is included in these three loading parameters.

Moreover, the supporting soil is subjected to the action of the inertial forces $\underline{F}$ that can be decomposed into a vertical and a horizontal component, $\underline{F}_v$ and $\underline{F}_h$ respectively. Let us emphasize that these forces are assumed to be uniform throughout the soil mass; an assumption to be discussed later on. From now on, the vertical component of the inertial forces $\underline{F}$ will be added to the unit weight of the soil and give rise to the modified unit weight:

$$\underline{\gamma}^* = \underline{\gamma} + \underline{F}_v = \gamma^* \underline{e}_z \tag{5}$$

with $\underline{e}_z$ the unit vector in the downward vertical direction. Concerning the influence of the unit weight on the ultimate loads, the classical demonstration is worth being recalled here, which starts from the static definition of the ultimate loads as the highest loads that can be equilibrated by a statically admissible stress field complying with the strength criteria. It turns out that any statically admissible stress field $\underline{\underline{\sigma}}^0$ in the case of the weightless soil provides a statically admissible stress field $\underline{\underline{\sigma}}^{\gamma^*}$ for the material with modified weight γ^* and vice versa, through the following equation:

$$\underline{\underline{\sigma}}^{\gamma^*} = \underline{\underline{\sigma}}^0 - \gamma^* z \underline{e}_z \otimes \underline{e}_z \tag{6}$$

These two stress fields equilibrate the same load on the foundation. If the classical Tresca strength criterion is concerned, they obviously comply with it at the same time. We also see that the same result holds with the Tresca strength criterion with no resistance to tension if γ^* is positive, which is true for the usual seismic excitations. It follows that in those cases γ^* does not influence the value of the ultimate loads supported by the footing.

Denoting by N, V, M and F_h the magnitudes of the corresponding vectors, we represent the loading parameters of the system by the loading vector:

$$\underline{Q} = (N,\ V,\ M,\ F_h) \tag{7}$$

The loading process is considered pseudo-static. No variation in time of the quantities in Eq. (7) is considered, since ultimate combinations of the loading parameters are sought.

We note finally that although no surface load at the soil surface is considered herein, the presented framework can accommodate the effect of a uniform vertical surface load $\underline{q}_v = q_v \underline{e}_z$ due to the additive character of the vertical surface load with respect to the vertical force N as explained by Salençon (1983). More specifically in the present case, if $\underline{Q}^0 = (N,\ V,\ M,\ F_h,\ 0)$ is supported by the foundation, then $\underline{Q}^{q_v} = (N + q_v A,\ V,\ M,\ F_h,\ q_v)$ is also supported by the foundation, A denoting the area of the footing, for positive values of q_v. It is clear, however, that consideration of the vertical component of surface load separately is devoid of any physical meaning in the context of earthquake loading. Since the surface load models the weight of overlying soil layers or adjacent structures, the horizontal component of the surface load should by no means be overlooked.

SOLUTION PROCEDURE

The kinematic approach of the Yield design theory is used to treat the problem. Following Salençon (2002), the procedure is briefly outlined:

a. In the domain Ω of the examined system (i.e. the foundation and the soil half-space), a virtual kinematically admissible (v.k.a.) velocity field $\underline{\hat{U}}$ is considered. This means, according to the usual continuum mechanics terminology, which we refer to here, that this vector field satisfies the boundary conditions on the velocity and is piecewise continuous and differentiable. It corresponds to a strain rate tensor $\underline{\underline{\hat{d}}}$ defined in Ω. It also corresponds to velocity jumps $[\underline{\hat{U}}]$ defined along jump surfaces Σ in Ω, which include the interface.

b. The resisting rate of work $\mathscr{P}_r(\underline{\hat{U}})$ developed in Ω by a stress tensor field $\underline{\underline{\sigma}}$ in the v.k.a. velocity field $\underline{\hat{U}}$ is given by the equation:

$$\mathscr{P}_r(\underline{\hat{U}}) = \int_\Omega \sigma_{ij} \hat{d}_{ij} d\Omega + \int_\Sigma \sigma_{ij} [\hat{U}_i] n_j d\Sigma \tag{8}$$

where σ_{ij} denote the components of $\underline{\underline{\sigma}}$ and n_j, the components of the unit vector normal to Σ. Summation over repeated indexes is implied throughout the paper. Given the v.k.a. velocity field $\underline{\hat{U}}$, the resisting rate of work $\mathscr{P}_r(\underline{\hat{U}})$ is maximized over all the stress fields that comply with the strength criteria of the soil and of the interface, through the introduction of the functions π, that represent the maximum resisting rate of work at a point in the domain. These are derived from the strength criteria as follows:

• *For the soil*:

$$\begin{cases} \pi(\underline{\underline{\hat{d}}}) = \sup \{\sigma_{ij} \hat{d}_{ij};\ \ f_{soil}(\underline{\underline{\sigma}}) \le 0\} \\ \pi(\underline{n}, [\underline{\hat{U}}]) = \sup \{\sigma_{ij} [\hat{U}_i] n_j;\ \ f_{soil}(\underline{\underline{\sigma}}) \le 0\} \end{cases} \tag{9}$$

• *For the interface*:

$$\pi(\underline{n}, [\underline{\hat{U}}]) = \sup \{\sigma_{ij}[\hat{U}_i]n_j; \quad f_{\text{interf}}(\underline{\sigma}) \leq 0\} \tag{10}$$

In Eqs. (9) and (10), f_{soil} and f_{interf} denote the strength criterion for the soil and for the interface respectively.

The explicit expression of the functions π, which are derived through duality from the strength criteria can be found in Salençon, (1983, 2002) for a series of strength criteria both for continuous media and for interfaces. The following are recalled for the needs of the problem considered herein:

• *Classical Tresca criterion (infinite tensile strength)*

$$\pi(\underline{\underline{\hat{d}}}) = \begin{cases} +\infty & \text{if} \quad \text{tr}\,(\underline{\underline{\hat{d}}}) \neq 0 \\ c(|\hat{d}_1| + |\hat{d}_2| + |\hat{d}_3|) & \text{if} \quad \text{tr}\,(\underline{\underline{\hat{d}}}) = 0 \end{cases} \tag{11}$$

$$\pi(\underline{n}, [\underline{\hat{U}}]) = \begin{cases} +\infty & \text{if} \quad [\underline{\hat{U}}] \cdot \underline{n} \neq 0 \\ c|[\underline{\hat{U}}]| & \text{if} \quad [\underline{\hat{U}}] \cdot \underline{n} = 0 \end{cases} \tag{12}$$

In the above, $\hat{d}_1$, $\hat{d}_2$ and $\hat{d}_3$ are the principal values of $\underline{\underline{\hat{d}}}$ and $\text{tr}\,\underline{\underline{\hat{d}}} = \hat{d}_1 + \hat{d}_2 + \hat{d}_3$.

• *Tresca criterion with zero tension "cut-off"*

$$\pi(\underline{\underline{\hat{d}}}) = \begin{cases} +\infty & \text{if tr}\,(\underline{\underline{\hat{d}}}) < 0 \\ c(|\hat{d}_1| + |\hat{d}_2| + |\hat{d}_3| - \text{tr}\,(\underline{\underline{\hat{d}}})) & \text{if tr}\,(\underline{\underline{\hat{d}}}) \geq 0 \end{cases} \tag{13}$$

$$\pi(\underline{n}, [\underline{\hat{U}}]) = \begin{cases} +\infty & \text{if} \quad [\underline{\hat{U}}] \cdot \underline{n} < 0 \\ c(|[\underline{\hat{U}}]| - [\underline{\hat{U}}] \cdot \underline{n}) & \text{if} \quad [\underline{\hat{U}}] \cdot \underline{n} \geq 0 \end{cases} \tag{14}$$

• *Tresca criterion for the interface without tensile strength*

$$\pi(\underline{n}, [\underline{\hat{U}}]) = \begin{cases} +\infty & \text{if} \quad [\underline{\hat{U}}] \cdot \underline{n} < 0 \\ c|[\underline{\hat{U}}] - ([\underline{\hat{U}}] \cdot n)n| & \text{if} \quad [\underline{\hat{U}}] \cdot \underline{n} \geq 0 \end{cases} \tag{15}$$

Thus, the maximum internal rate of work $\mathscr{P}_{\text{mr}}(\underline{\hat{U}})$ is given by:

$$\mathscr{P}_{\text{mr}}(\underline{\hat{U}}) = \int_{\Omega} \pi(\underline{\underline{\hat{d}}}) \text{d}\Omega + \int_{\Sigma} \pi(\underline{n}, [\underline{\hat{U}}]) \text{d}\Sigma \tag{16}$$

c. Given the velocity field $\underline{\hat{U}}$ and for all the loading parameters Q_i, the associated kinematic parameters $\dot{q}_i(\underline{\hat{U}})$ are determined directly by the velocity field and the rate of external work can thus be computed as follows:

$$\mathscr{P}_{\text{ext}}(\underline{\hat{U}}) = Q_i \dot{q}_i(\underline{\hat{U}}) \tag{17}$$

d. Since the resisting rate of work in Eq. (8) is maximized through the π-functions it follows from the principle of virtual rates of work that the fundamental inequality should be satisfied:

$$\mathscr{P}_{\text{ext}}(\underline{\hat{U}}) \leq \mathscr{P}_{\text{mr}}(\underline{\hat{U}}). \tag{18}$$

The equality in Eq. (18) yields upper bound estimates for the ultimate loads of the structure.

e. Through the examination of a series of v.k.a. velocity fields, the minimum upper bound is retained as the most satisfactory approximation to the exact solution.

Relevant velocity fields. Any v.k.a. velocity field may be used in the above procedure but it comes out obviously that only those v.k.a. velocity fields for which $\mathscr{P}_{\text{mr}}(\underline{\hat{U}})$ remains finite shall lead to a valuable upper bound estimate of the extreme loads. This condition implies that the functions π defining $\mathscr{P}_{\text{mr}}(\underline{\hat{U}})$ must be kept finite at any point in the system. Such so-called *relevant* virtual velocity fields must comply with conditions on $\underline{\underline{\hat{d}}}$ and $(\underline{n}, [\underline{\hat{U}}])$, which are mathematically derived from Eqs. (11)–(15), that is just from the strength criteria without any physical significance as a constitutive law or a flow rule. They are sometimes called kinematically admissible in the literature, which is somewhat misleading since the condition comes from the material strength criterion and not from the geometry of the problem.

Obviously, it comes out that a relevant virtual velocity field for the classical Tresca criterion is also relevant for the Tresca criterion without tensile strength, but not vice versa.

Virtual failure mechanisms as sets of virtual velocity fields. An exhaustive examination of all v.k.a. velocity fields is neither possible nor necessary from a practical point of view: only satisfactory upper bounds need to be established. To this end, a series of v.k.a. velocity fields is investigated. It is clear that each v.k.a. velocity field corresponds to a particular virtual mechanism of bearing capacity failure of the soil-foundation system. The virtual failure mechanisms considered are grouped in *classes* of mechanisms corresponding to a particular bearing failure pattern depending on a number of geometrical parameters which define the shape of the mechanism. The optimization procedure outlined in steps (*a*)–(*e*) results in finding those values of the geometrical parameters *in each class* that give rise to the optimal upper bounds and then selecting the minimum among the minima derived from those classes of mechanisms.

BASIC ASSUMPTIONS

Uniform horizontal inertial forces in the soil. As already stated the assumption is made that the horizontal inertial forces $\underline{F}_{\text{h}}$ developing in the soil volume are uniform in space. Qualitatively, in order for such an assumption to be valid, the failure mechanism has to be shallow with respect to the depth of the supporting soil layer in which the seismic waves are propagating. Pecker and Salençon (1991) suggested that, denoting by d and D respectively the failure mechanism thickness and the depth of the soil layer, the following condition should be satisfied: $d/D < 1/10$. In general, if it is expected that the variation of the horizontal inertial forces near the ground

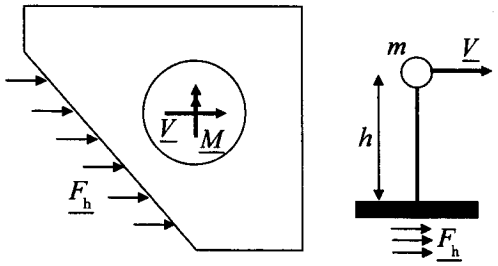

Fig. 7. Collinear loading parameters on the footing, justified by the consideration of a SDOF superstructure

surface is significant, a more sophisticated profile for $\underline{F_h}$ should be adopted.

Collinear loading parameters. We will consider that $\underline{V}$ and $\underline{F_h}$ are collinear while $\underline{M}$ is perpendicular to their direction as presented in Fig. 7. As a matter of fact, this choice corresponds to the excitation of a single-degree-of-freedom (SDOF) superstructure, for which $\underline{V}$ is collinear with $\underline{F_h}$ and the moment is expressed by the product $M=Vh$, where h is the height of the SDOF superstructure. However, the collinearity of the loading parameters remains valid for a multi degree of freedom superstructure under specific conditions.

CLASSES OF VIRTUAL FAILURE MECHANISMS

Planar non plane strain mechanisms. Following Puzrin and Randolph (2003a, b) we may characterize the virtual mechanisms under consideration as planar non plane strain ones. The term "planar" refers to the fact that the velocity field is such that a Cartesian coordinate system (x, y, z) may be defined, in which the velocity component parallel to an axis is zero: e.g. $\hat{U}_y=0$ as it is presented in Fig. 8. The term "non plane strain" refers to the fact that the two non zero components of the velocity remain functions of the three coordinates (x, y, z). Similar velocity fields have been used by Cuvillier (2001) and Subrin and Wong (2002) for the study of the stability of a tunnel face by the kinematic approach of the Yield Design theory. Such velocity fields are treated herein using the theoretical methodology recently proposed by Puzrin and Randolph (2003a, b). The key idea of this methodology is a coordinate transformation from the original to a new curvilinear coordinate system, such that only one component of the velocity does not vanish (e.g., $\hat{U}_x \neq 0$):

$(x, y, z) \rightarrow (x', y', z')$ such that:

$$\hat{U}_{y'}=\hat{U}_{z'}=0 \text{ and } \hat{U}_{x'}=f(x', y', z') \qquad (19)$$

The coordinate transformation in Eq. (19), combined with the conditions of relevance for the Tresca strength criterion, leads to a significant simplification of the tensorial quantities (elements of $\underline{\underline{\hat{d}}}$) required for the evaluation of the π-functions and for the determination of the maximum resisting rate of work in the system.

Class of translational mechanisms. This pattern of bearing failure was originally proposed by Green (1954) for combined shear and pressure plane strain problems. It was adapted to a rigid circular footing by Puzrin and Randolph (2003b) by considering that the width of the mechanism in a cross-section by a vertical plane is proportional to the width of the footing in the same cross-section (c.f., Fig. 9). The mechanisms are named "translational" as the footing translates with a virtual velocity $\underline{\hat{U}_0}$. This velocity is constant in magnitude along the streamlines of the mechanism. The shape of each virtual mechanism of failure is defined by the two angles δ and ε. Allowable values for these parameters are:

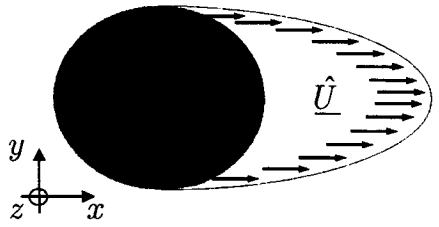

Fig. 8. Planar, non plane strain virtual velocity fields

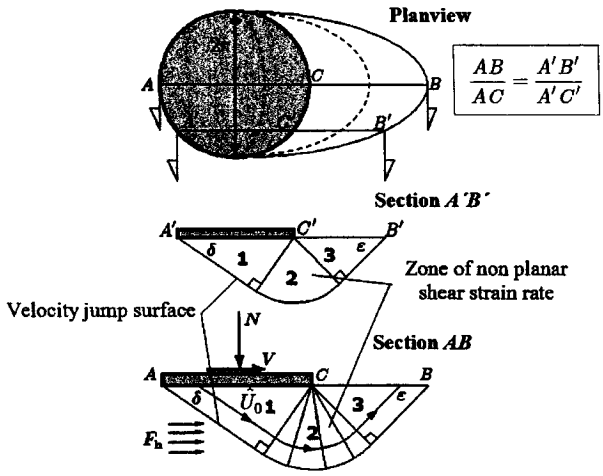

Fig. 9. The class of translational mechanisms: Planview and longitudinal vertical sections

$$0<\delta<\frac{\pi}{2}, \quad 0<\varepsilon<\frac{\pi}{2}.$$

The mechanisms exhibit three zones within the soil mass, presented in Fig. 9. Zones 1 and 3 translate rigidly with velocity $\underline{\hat{U}_0}$ while zone 2 is a region where non-plane shear strain rate is developed. Contributions to the maximum resisting rate of work for this class are developed within the volume of zone 2 and along the velocity jump surface in the soil. The mechanisms involve no uplift of the footing. Since this class of virtual mechanisms does not imply any rotation of the footing, the upper bound estimates it provides through Eq. (17) do not involve the moment M.

Class of purely rotational mechanisms. The plane strain version of this class of mechanisms was studied by Salençon and Pecker (1995a, b). Segikuchi and Kobayashi (1997) extended the mechanisms for a circular footing subjected to an eccentric vertical load (action of N and M). Herein, the configurations studied by Segikuchi and Kobayashi (1997) are extended in order to include a horizontal force V and horizontal inertial forces F_h in the soil. The rigid circular footing is considered to rotate rigidly around an axis of rotation as depicted in Fig. 10. The rotation of the footing induces rigid rotational failure of the soil below with a virtual angular velocity $\hat{\omega}$. The shape of each mechanism in the class is defined by two geometrical parameters: κ and λ. Two distinct failure patterns are obtained depending on the value of the parameter λ; For $1<\lambda<2$, there is no uplift of the

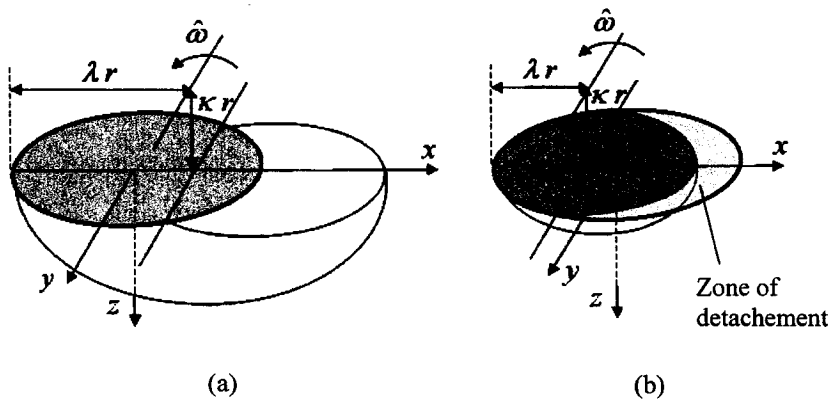

Fig. 10. The class of purely rotational mechanisms (a) without detachment and (b) with detachment at the soil-foundation interface

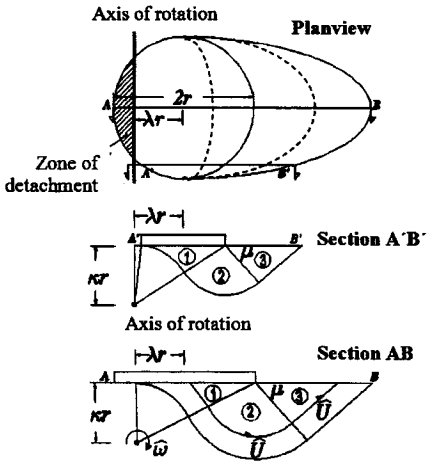

Fig. 11. The class of shear rotational mechanisms; Configuration with a small zone of detachment at the soil-footing interface. Planview and longitudinal vertical sections

footing with respect to the soil surface and the maximum resisting rate of work is only produced along the velocity jump surface within the soil volume. For $0<\lambda<1$, uplift of the footing with respect to the soil surface takes place and a fraction of the maximum resisting rate of work is developed on the zone of soil-footing detachment.

Class of shear-rotational mechanisms. The geometry of the "shear-rotational" mechanisms is presented in Fig. 11. This failure pattern was originally proposed by Brinch Hansen (1953) for the study of active earth pressures. Salençon and Pecker (1995a, b) presented a variation of this mechanism adapted to the bearing capacity problem of a strip footing under an inclined and eccentric load (N, V, M). A similar mechanism was also studied by Randolph and Puzrin (2003) for a circular footing configuration exhibiting perfect adhesion at the soil-foundation interface. Bearing failure is induced by rotation of the footing around an axis of rotation, which is located within the soil mass. The shape of mechanisms in the class is defined by three geometrical parameters: κ, λ and the angle μ. The mechanisms are named "shear-rotational" to be distinguished from the purely rotational ones, since development of non planar shear strain rate occurs in the zones 2 and 3 within the soil volume. By changing the position of the axis of rotation with respect to the footing, three separate configurations are obtained: a) with a small zone of detachment (c.f., Fig. 11), b) without detachment (c.f., Fig. 12(a)) and c) with a large zone of detachment (c.f., Fig. 12(b)). For this family of mechanisms, contributions to the maximum resisting rate of work are developed within the soil volume in the zones 2 and 3, along the velocity jump surface in the soil mass and on the zone of soil-footing detachment in the case of uplift.

KEY ASPECTS OF THE SOLUTION PROCEDURE

Rate of work of the external forces. Since the circular footing is assumed to be perfectly rigid, any v.k.a. velocity field $\underline{\hat{U}}$ is due to comply with a rigid body motion of the footing as a boundary condition. For planar velocity fields, assuming $\hat{U}_y=0$, such a rigid body motion is defined by the virtual rate of rotation $\hat{\omega}$ and the two components $\hat{U}_{O,x}$, $\hat{U}_{O,z}$ of the virtual velocity of the center O of the footing. It follows that the complete expression for the rate of work of the external forces is:

$$\mathscr{P}_{\text{ext}}=N\hat{U}_{O,z}+V\hat{U}_{O,x}+M\hat{\omega}+F_{\text{h}}\int_{\Omega}\underline{\hat{U}}\cdot\underline{e}_x\,\mathrm{d}\Omega \qquad (20)$$

Use of Tresca criterion with and without tensile strength. The considered v.k.a. velocity fields satisfy the conditions of relevance for the classical Tresca strength criterion and consequently, for the Tresca strength criterion with a zero tension "cut-off". There is no difference in the use of the two criteria as far as the maximum resisting rate of work is concerned within the soil volume and along the velocity jump surfaces in the soil mass. The only difference arises from the calculation of the maximum resisting rate of work on the areas of foundation uplift, where the soil strength criterion is combined with the strength criterion of the interface itself. Obviously (Salençon, 1983) the upper bound estimates in the case of the Tresca criterion with a zero tension cut-off are expected to be lower than or equal to the ones obtained in the case of the full Tresca criterion. This difference is observed when the optimal virtual failure mechanism ex-

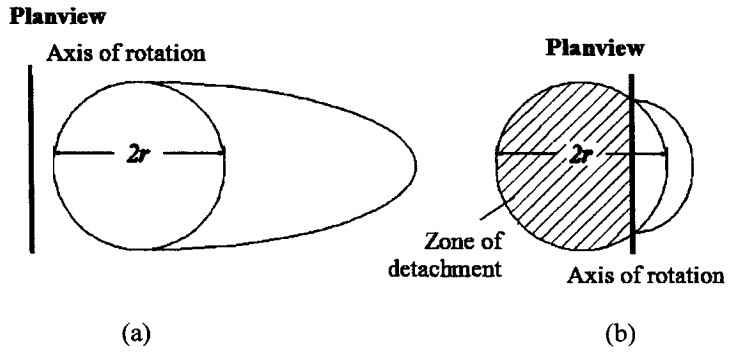

Fig. 12. Shear rotational mechanisms; Planviews of (a) configuration without detachment and (b) configuration with a large zone of detachment at the soil-foundation interface

hibits a zone of uplift of the footing.

Optimization procedure. An important part of the solution procedure is the optimization of the virtual failure mechanisms in order to obtain the minimum upper bounds for the ultimate loads supported by the system. For each separate geometrical configuration of the considered classes of virtual mechanisms (1 configuration for the translational mechanisms, 2 for the purely rotational and 3 for the shear rotational ones), an optimization problem is solved. It concerns the minimization of a nonlinear objective function depending on a number of *bounded* variables, namely the geometrical parameters used to define the shape of each geometrical configuration (2 variables for the translational and the purely rotational mechanisms and 3 variables for the shear-rotational mechanisms). The problem was solved on a commercial platform for scientific computing with an algorithm using a robust interior trust region approach (Coleman and Li, 1996).

RESULTS

Dimensionless parameters. The interpretation of the results is made easier through the introduction of a set of dimensionless parameters derived from the geometrical, loading and strength parameters that define the problem, namely:

$$N=\frac{N_{Ed}}{C_0\pi r^2},\ V=\frac{V_{Ed}}{C_0\pi r^2},\ M=\frac{M_{Ed}}{2C_0\pi r^3},\ F_h=\frac{r\rho a_h}{C_0\pi} \qquad (21)$$

and

$$k=\frac{rG}{C_0} \qquad (22)$$

where the index "Ed" refers to the values adopted for Earthquake design. The definition of the dimensionless F_h involves the soil mass density ρ together with a horizontal acceleration a_h characteristic of the considered earthquake, which can be, for instance, the peak ground horizontal acceleration (PGHA).

The latter parameter k expresses the degree of heterogeneity in the system. For a homogeneous soil layer, $k=0$. Common values of r, G and C_0 lead to the range $0\leq k\leq 3$.

Table 1. Values of the critical F_h as function of k

Class of mechanisms	critical value of F_h			
	$k=0$	$k=0.5$	$k=1$	$k=3$
Translational	1.32	1.80	2.29	4.05
Purely rotational	0.99	1.28	1.54	2.45
Shear rotational	0.66	0.90	1.15	2.03
MINIMUM	0.66	0.90	1.15	2.03

Critical F_h. In principle, failure of the system may be induced just by the action of the soil inertial forces, even for very small values of the vertical, horizontal and moment loads. This idea gives rise to the notion of *critical* F_h, which is defined as the maximum horizontal inertial volume force in the soil supported by the system, when the other loading parameters are zero: ($N=0$, $V=0$, $M=0$). Table 1 summarizes the calculated values of *critical* F_h for the classes of mechanisms examined, as a function of k, the degree of heterogeneity of the system. The values in Table 1 reveal an important increase of the critical value of F_h with increasing k. The minimum value is equal to $F_h=0.66$ and is obtained through a shear-rotational mechanism. For homogeneous soils and usual values of the other parameters, this value of F_h corresponds to a very strong earthquake (e.g., $a_h=10$ m/sec$^2=1$ g for $r=4$ m, $C_0=40$ kPa, $\rho=20$ kN/m^3). Even so, it can be noted, that this value is obtained by a mechanism with very large dimensions with respect to the footing width that has no physical meaning whatsoever. It is understood that for practical applications, the value of F_h will turn out to be smaller than the critical one. Nonetheless, if this condition is violated it means that the method cannot describe the overall process of seismic loading of the footing sufficiently and that a more realistic description of seismic excitation should be retained.

Presentation of the results. The upper bounds for the ultimate loads supported by the foundation are represented as surfaces in the space of the loading parameters (N, V, M) for different values of F_h and k. A simplified sketch of such a surface is given in Fig. 13. Several interesting points can be noted:

i. The point of intersection of the surface with the axis of vertical forces N corresponds to the maximal vertical force supported by the footing (N_{max}). If additionally $F_h = 0$, this value is the static bearing capacity of the foundation under centered vertical loading, denoted by N^0_{max}. For the examined configurations, N^0_{max} is known *exactly* (*see*, for example, Salençon and Matar, 1982) and can help investigate the error induced by the upper bounds established herein.

ii. For $M=0$, two symmetric branches are obtained by the intersection of the "ultimate surface" with the (N, V) plane. The optimal upper bounds along these branches are mainly obtained by translational mechanisms. These branches are symmetric since the problem with N, V and F_h only, is symmetric with respect to sign inversion of V and F_h.

iii. For non-zero values of M, one part of the ultimate surface is obtained from shear-rotational mechanisms and the other part from purely rotational mechanisms. The ultimate surface is not symmetric with respect to the plane $V=0$.

iv. The region that corresponds to quasi-axisymmetric configurations of loading appears not to be sufficiently described by the mechanisms considered, which may come from the fact that they are unilateral. Anyway, such configurations of loading do not present a great interest when earthquake loadings are concerned, since the latter imply significant horizontal forces and moments acting on the footing. It can be expected (without rigorous proof) that the error induced by the established upper bounds is maximum in the region of the ultimate surface that corresponds to quasi-axisymmetric configurations of loading.

In the following, the results refer to the more realistic Tresca criterion with a zero tension "cut-off" for the soil strength, unless otherwise stated. Several diagrams are presented that can be viewed as sections of the "ultimate surface" in the (N, V, M) space. The curves represent the bounds for the ultimate combinations of the loading parameters and indicate the class of mechanisms from which each bound is obtained. This is done by assigning a specific symbol for each class. The symbols used in the diagrams are summarized in Table 2. We note that the only configuration that yields no optimal upper bounds is the shear rotational mechanism with no uplift.

Interaction diagram **(N, V, $M=0$, F_h).** The diagrams in Fig. 14 present the relation between the ultimate horizontal and vertical force for $k=0$ and $k=1$ and for three different values of F_h. The maximum value for V is 1, corresponding to a translational mechanism of failure by

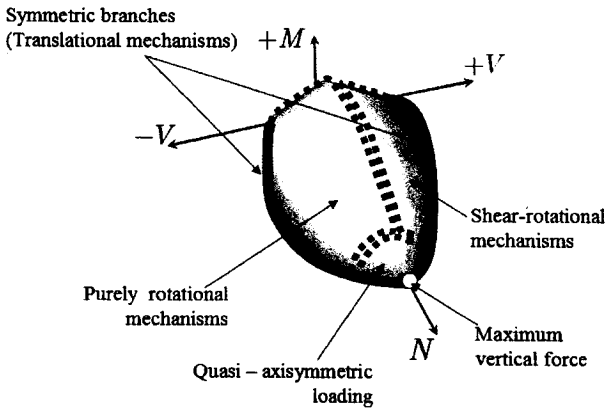

Fig. 13. Simplified sketch of ultimate surface in the space (N, V, M)

Table 2. Symbols representing the different classes of mechanisms in the result diagrams

Translational	◇
Purely Rotational–No uplift	●
Purely Rotational–With uplift	▲
Shear Rotational–Small uplift zone	■
Shear Rotational–Large uplift zone	*
Exact values	○

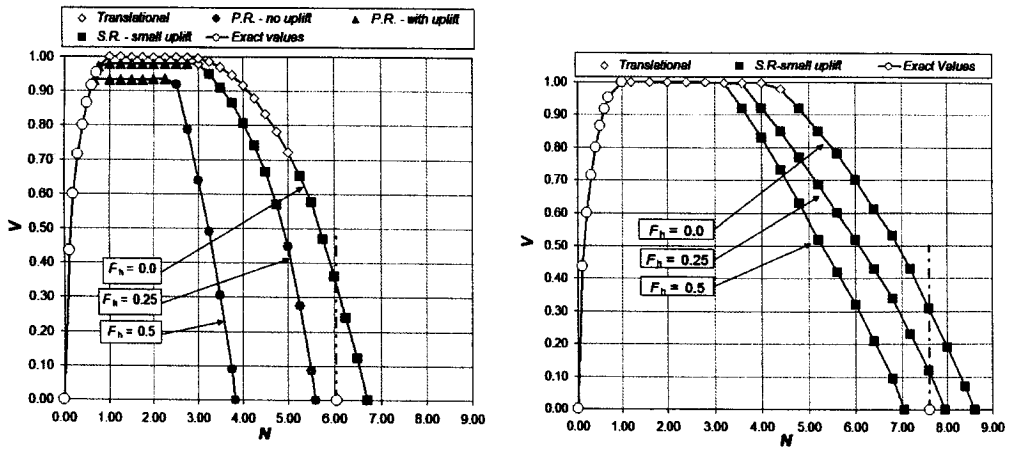

(a) (b)

Fig. 14. Interaction diagram (N, V, $M=0$, F_h). Tresca criterion with zero tension "cut-off". a) $k=0$ and b) $k=1$

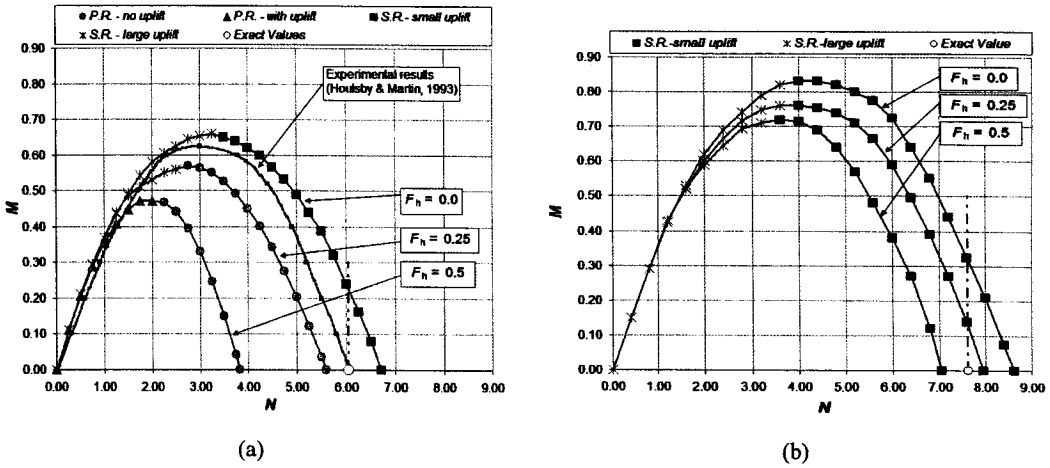

Fig. 15. Interaction diagram (N, $V=0$, M, F_h) and experimental results by Houlsby and Martin (1993). Tresca criterion with zero tension "cut-off". a) $k=0$ and b) $k=1$

pure sliding along the soil-footing interface, if $F_h=0$.

It is also interesting to note that for $F_h>0$, the purely rotational mechanism gives a better optimal upper bound than the pure sliding one. The depth of this mechanism is relatively small, so that it is very close to a pure sliding, but nevertheless it incorporates a contribution of F_h to the rate of work of the external forces. This phenomenon is less pronounced for larger values of k as revealed by the diagram for $k=1$. Another interesting observation is that the effect of F_h remains negligible as long as $N^0_{max}/N>2.5$. It becomes more important when N increases and especially when $N^0_{max}/N<2$. This is true both for $k=0$ and $k=1$. However, for $k=1$, the negative effect of a high F_h is reduced. This observation emphasizes the favourable effect of a cohesion gradient which, not only increases the global system strength, but also reduces the relative adverse effect of F_h.

***Interaction diagram* (N, $V=0$, M, F_h).** By setting $V=0$, we obtain optimal upper bounds for the ultimate combinations of M and N, represented in Fig. 15 for $k=0$ and $k=1$. From the paper by Houlsby and Martin (1993) experimental data are available in the case $k=0$, $F_h=0$, which are plotted in Fig. 15(a)) for comparison. It comes out that the upper bounds are satisfactory, from a practical point of view, and that the difference is larger for the larger values of N that correspond, as it was explained, to quasi-axisymmetric loading configurations. For small values of N, the optimal upper bounds are obtained by mechanisms with a significant zone of uplift of the footing, which is not the case as N increases. The effect of F_h follows the same behaviour as in Fig. 14 (interaction V, N). The practical significance of this observation is that a factor of safety against permanent loads (expressed by the ratio N^0_{max}/N) larger than 2.5 can guarantee that the effect of soil inertial forces is negligible, even for very strong earthquakes. On the contrary, for a safety factor against permanent loads smaller than 2 it is necessary to take these forces into account for the earthquake-resistant design of shallow foundations. Such conclusions are in agreement both with observations of real foundation bearing capacity failures, mainly after the Guerrero-Michoacán earthquake (Mexico, 1985) as presented by Mendoza and Auvinet (1988) and with the existing theoretical results for strip and rectangular footings (c.f., Pecker and Salençon, 1991); Paolucci and Pecker, 1997a).

***Interaction diagram* ($N=const.$, V, M, F_h).** For a fixed value of the vertical force N, the interaction between ultimate values of M and V is obtained. In Fig. 16, two plots are presented ($k=0$) for $N^0_{max}/N=3$ (corresponding to a proper foundation design) and $N^0_{max}/N=1.5$ (unconservative design). This diagram presents a significant practical usefulness: if the geometrical and rigidity characteristics of the superstructure are known, a relationship between the resultant moment and the horizontal force (base shear force) on the footing can be established. For example, in the simple case of a SDOF superstructure, this relationship is simply: $M=Vh$. Such a relationship defines a loading path in the (M, V) plane allowing for the determination of the ultimate combination of M and V for given N and F_h. Such trajectories are presented in Fig. 16. The two diagrams highlight the significant decrease of the bearing capacity with increasing F_h for $N^0_{max}/N=1.5$. Even for $V=0$, $M=0$, a value $F_h=0.5$ cannot be supported by the footing.

Another interesting remark, is the fact that the part of the diagram obtained from purely rotational mechanisms ($V<0$), corresponds to SDOF structures with a negative height h. For loads that originate from the inertial response of a superstructure, such a case presents limited physical sense.

It is noted finally that in this diagram, the values of F_h reflect the *magnitude* of the horizontal inertial volume forces but not necessarily the sign of their direction. The inertial forces are deemed to be directed in the same direction as V and always act in an unfavourable way in the creation of the failure mechanism, *i.e.* their contribution has always a positive sign in the expression of the rate of work of the external forces. This is justified by noting that a seismic bearing capacity failure is actually driven

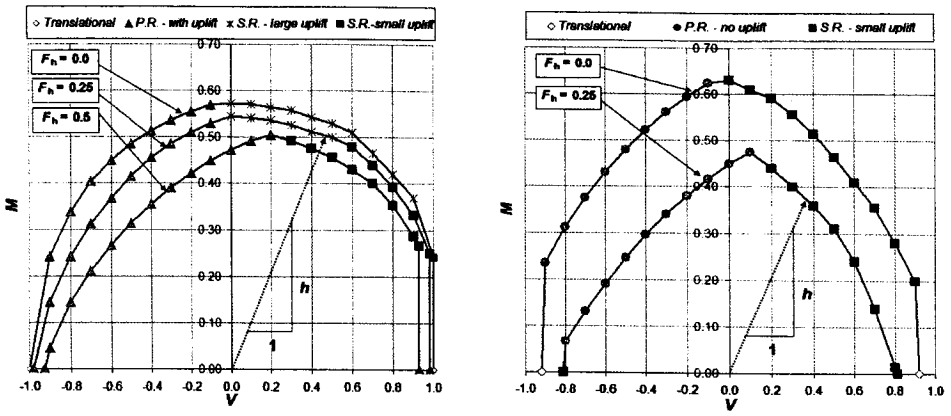

Fig. 16. Interaction diagram (N = const., V, M, F_h). Tresca criterion with zero tension "cut-off" and $k = 0$. a) $N = 1/3\ N^0_{max}$ and b) $N = 2/3\ N^0_{max}$. Ultimate loading paths for $F_h = 0.25$ in a SDOF superstructure

by the earthquake excitation of the soil-foundation system.

Soil with and without tensile strength. As it has been explained, for the examined v.k.a. failure mechanisms, the only difference between the two soil criteria considered herein concerns the maximum resisting rate of work developing in the zone of soil-footing detachment. Therefore optimal upper bounds obtained from a virtual mechanism of failure exhibiting foundation uplift are slightly smaller in the case of a Tresca criterion with a zero tension "cut-off" than with the classical Tresca criterion. The difference between the results obtained with the two criteria is expected to increase for regions of the ultimate surface corresponding to failure mechanisms with a significant zone of foundation uplift. These are the regions that correspond to small N and large M, V loading (high eccentricity and inclination of the load). In Fig. 17, results obtained with the two criteria are compared in the (M, V) interaction diagram for $N^0_{max}/N = 3$ and $k = 0$. The diagram reveals that the difference is quite important and thus the use of the classical Tresca criterion for loadings with high values of M, V accompanied by small values of N should be looked at very carefully.

Assessment of the error induced by the upper bounds. The solutions established in this study are optimal upper bounds of the ultimate loads supported by the foundation. They are thus *unconservative*. With this in mind, it is helpful to evaluate how much the solutions presented differ from the exact solutions. This can be done, for example, for the static bearing capacity of the footing under centered vertical loading, which is known *exactly*. This means that for this loading configuration, it has been feasible to construct a *complete* statically admissible stress field and an associated kinematically admissible velocity field. Here, the exact solutions of Salençon and Matar (1982) are compared with the optimal upper bounds for a range of values for k. Figure 18 presents the results. The optimal upper bound is obtained by a shear rotational mechanism with a small area of foundation uplift. The error increases from approximately 11% for a

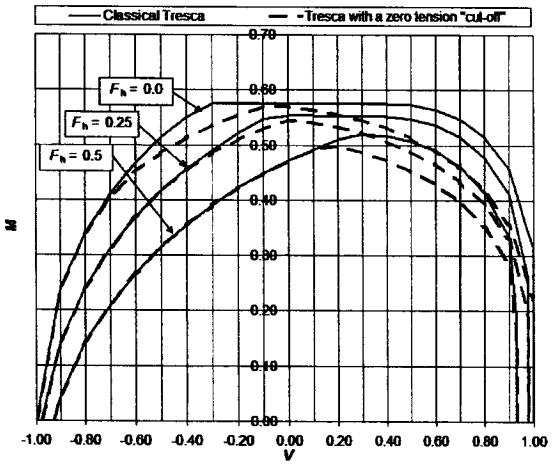

Fig. 17. Comparison between classical Tresca and Tresca criterion with a zero tension "cut-off". Interaction diagram ($N = 1/3\ N^0_{max}$, V, M, F_h) and $k = 0$

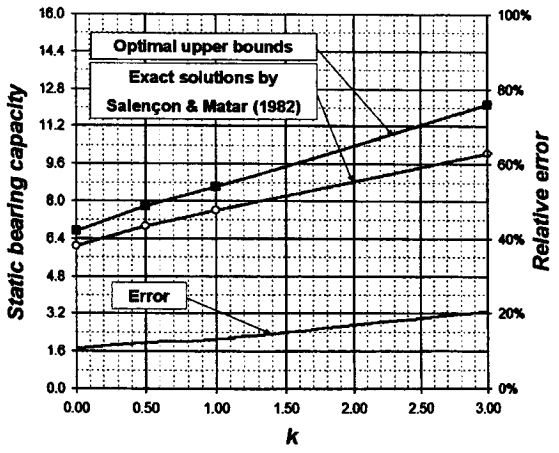

Fig. 18. Comparison between optimal upper bounds and exact solutions (Salençon and Matar, 1982) for the static bearing capacity of a circular footing on a heterogeneous soil

homogeneous soil up to approximately 20% for a strongly heterogeneous soil. It is recalled that these values reflect the maximum error induced by the optimal upper bounds since the mechanisms chosen (unilateral mechanisms) are more suitable for loadings with significant M, V and F_h.

Adaptation of the EC8 expression for circular footings. Finally, an adaptation of the Eurocode 8 expression is proposed so that it can be used also for strip and circular footings on homogeneous or heterogeneous cohesive soils. The expression of the Eurocode 8 for strip footings is written as follows:

$$\frac{(1-e\bar{F}_h)^{c_T}(\beta\bar{V})^{c_T}}{(\bar{N})^a[(1-m\bar{F}_h^{c_N})^{c'_N}-\bar{N}]^b}+\frac{(1-f\bar{F}_h)^{c_M}(\gamma\bar{M})^{c_M}}{(\bar{N})^c[(1-m\bar{F}_h^{c_N})^{c'_N}-\bar{N}]^d}-1\le 0 \tag{23}$$

subjected to the constraints:

$$0<\bar{N}\le(1-m\bar{F}_h^{c_N})^{c'_N},\ |\bar{V}|\le\frac{1}{\pi+2}.$$

In Eq. (23), we define:

$$\bar{N}=\frac{N_{Ed}}{N^0_{max}},\ \bar{V}=\frac{V_{Ed}}{N^0_{max}},\ \bar{M}=\frac{M_{Ed}}{BN^0_{max}},\ \bar{F}_h=\frac{\rho a_h B}{c}$$

$$N^0_{max}=(\pi+2)cB$$

The values of the other parameters in Eq. (23) are presented in Table 3. These are constant numerical parameters that were obtained by Pecker (1997) using a procedure of curve fitting to theoretical results of the seismic bearing capacity of strip footings.

As it was said, this expression has been established and therefore is valid for *strip* footings of width B resting on *homogeneous* cohesive soils with cohesion c. For application to circular footings, the proposed modification consists in replacing the value of N^0_{max} for strip footings by the corresponding value for circular ones, which is known as: $N^0_{max}=6.05c\pi r^2$ (Eason and Shield, 1960). Moreover, for use of Eq. (23) the value of $\bar{F}_h$ needs to be updated as follows: $\bar{F}_h=\pi F_h$, with F_h calculated for circular footings as in Eq. (21). Concerning the Eurocode 8 expression and its modification, it is noted that the ultimate surface described by Eq. (23) is symmetric with respect to the plane $V=0$, which is not the case for the optimal upper bounds established herein. Figure 19 presents the (M, V) interaction diagrams for $N^0_{max}/N=3$ and $N^0_{max}/N=1.5$ as obtained by the upper bounds and the modified Eurocode 8 expression. The agreement of the two families of curves is very satisfactory mainly for the part $M>0$, $V>0$, which corresponds to physically realistic combinations of loads. The good agreement of the two curve families is in line with the hypothesis (*see* also, Bransby and Randolph, 1998) that the shape of the ultimate surface for strip and circular footings is very similar and that its size is controlled by the value of N_{max}. This is verified herein even in the presence of F_h.

For strip or circular footings on heterogeneous soils, further modification is required to account for the inhibitory role of the vertical cohesion gradient G on the negative effect of F_h. The proposed modification consists in considering that the soil-footing system exhibiting strength parameters (C_0, $G\neq 0$) is replaced by a system

Table 3. Values of constant numerical parameters in Eq. (23)

a	0.70	c_N	1.22
b	1.29	c'_N	1.00
c	2.14	c_T	2.00
d	1.81	c_M	2.00
e	0.21	c'_M	1.00
f	0.44	β	2.57
m	0.21	γ	1.85

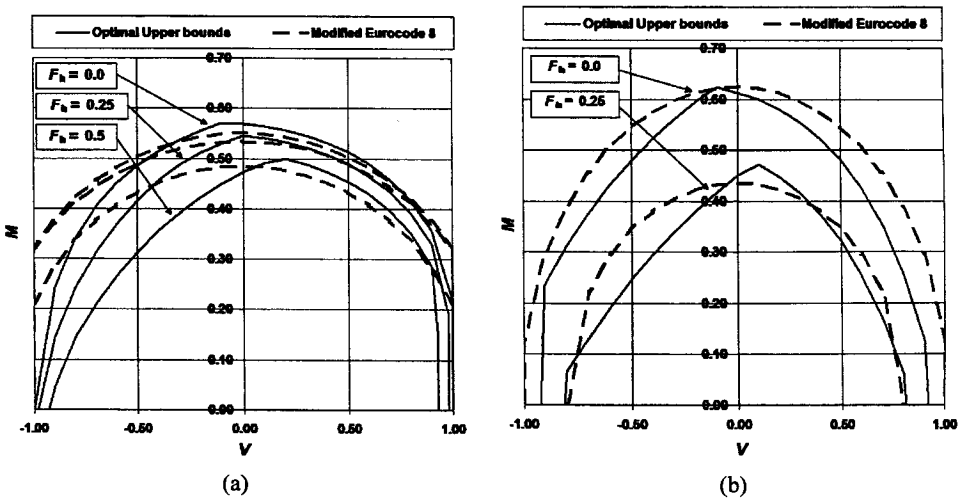

Fig. 19. Comparison between optimal upper bounds and ultimate loads obtained by the modified EC8 expression. Interaction diagram (N = const., V, M, F_h). Tresca criterion with zero tension "cut-off" and $k=0$: a) $1/3\,N^0_{max}$ and b) $N=2/3\,N^0_{max}$

with strength parameters (C_0, $G=0$), which is subjected to *reduced* inertial volume forces F'_h. It is proposed that the reduced inertial forces are given by:

$$\bar{F}'_h=\left(\frac{N^0_{max|0}}{N^0_{max|G}}\right)\bar{F}_h \tag{24}$$

with $\bar{F}_h=(\rho a_h B/C_0)$ for strip and $\bar{F}_h=(r\rho a_h/C_0)$ for circular footings respectively.

In Eq. (24), $N^0_{max|0}$ and $N^0_{max|G}$ are the static bearing capacities of a homogeneous (C_0, $G=0$) and a heterogeneous (C_0, $G\neq 0$) soil respectively. These quantities have been given for strip and circular footings by Salençon and Matar (1982). The other parameters for application of Eq. (23) are given by:

$$\bar{N}=\frac{N_{Ed}}{N^0_{max|G}},\ \bar{V}=\frac{V_{Ed}}{N^0_{max|0}},\ \bar{M}=\frac{M_{Ed}}{BN^0_{max|G}}\ \text{(strip)},$$

$$\bar{M}=\frac{M_{Ed}}{2rN^0_{max|G}}\ \text{(circular)}$$

Note that N and M are normalized with respect to $N^0_{max|G}$ whereas V is normalized with respect to $N^0_{max|0}$. This is because the ultimate value of V is controlled uniquely by C_0 while the presence of a nonzero G has no effect on it whatsoever. Also note that in the above adaptation of Eq. (23) to heterogeneous soil conditions, the shape of the ultimate surface is preserved, which is not true in general as it has been revealed by Gouvernec and Randolph (2003). However, by considering that the change in the shape of the ultimate surface is negligible, the proposed modification offers a quick extension of Eq. (23) to circular footings and heterogeneous soil conditions without recalibration of the numerical parameters or modification of the general format of Eq. (23).

Table 4 summarizes the definition of the different parameters for use of the analytical expression of the EC8 in the cases of strip and circular footings on homogeneous and heterogeneous cohesive soils.

The optimal upper bounds are compared with the ultimate loads as obtained by the modified Eurocode 8 expression in Fig. 20, where the interaction diagrams (M, V) for $N=1/3\ N^0_{max|G}$ and $k=1$, $k=3$ are presented. It is revealed that the two families of curves exhibit a satisfactory agreement and that the modified Eq. (23) can be used as a quick estimate of the ultimate loads on the footing. Attention should be paid however to the particular load combinations that *violate* the established upper bounds given by Eq. (23). These correspond mainly to loading with large N combined with large V (c.f., Fig. 19(b)).

CONCLUSIONS

Optimal upper bounds have been established for the ultimate seismic loads supported by a circular footing resting on the surface of a purely cohesive soil with a vertical cohesion gradient. These bounds are deemed to be acceptable, from a practical point of view, especially for small to moderate values of the vertical gradient of the cohesion. The results revealed that the effect of the horizontal inertial forces in the soil volume is, in general, negligible as long as the vertical force on the footing remains smaller than one third of its static bearing capacity. Moreover, it was pointed out that the Eurocode 8 expression describing the seismic bearing capacity of a strip footing on homogeneous soil can be satisfactorily extended to circular footings and heterogeneous soils with very small modifications. Finally, it is emphasized that the corpus of results established herein should necessarily be enriched by other solutions (mainly lower bound solutions) or by experimental results, since the established

Table 4. Definition of parameters for use of Eq: (23). The index "Ed" denotes the values chosen for earthquake design of the footing

	HOMOGENEOUS COHESIVE SOIL (G_0, $G=0$)		HETEROGENEOUS COHESIVE SOIL (G_0, G)	
PARAMETER	STRIP	CIRCULAR	STRIP	CIRCULAR
$N^0_{max\|0}$	$(\pi+2)C_0B$	$6.05C_0\pi r^2$	$(\pi+2)C_0B$	$6.05C_0\pi r^2$
$N^0_{max\|G}$	—	—	*cf.* Salençon and Matar (1982)	
$\bar{N}$	$\frac{N_{Ed}}{N^0_{max\|0}}$	$\frac{N_{Ed}}{N^0_{max\|0}}$	$\frac{N_{Ed}}{N^0_{max\|G}}$	$\frac{N_{Ed}}{N^0_{max\|G}}$
$\bar{V}$	$\frac{V_{Ed}}{N^0_{max\|0}}$	$\frac{V_{Ed}}{N^0_{max\|0}}$	$\frac{V_{Ed}}{N^0_{max\|0}}$	$\frac{V_{Ed}}{N^0_{max\|0}}$
$\bar{M}$	$\frac{M_{Ed}}{B\,N^0_{max\|0}}$	$\frac{M_{Ed}}{2r\,N^0_{max\|0}}$	$\frac{M_{Ed}}{B\,N^0_{max\|G}}$	$\frac{M_{Ed}}{2r\,N^0_{max\|G}}$
$\bar{F}_h$	$\frac{\rho a_h B}{C_0}$	$\frac{\rho a_h r}{C_0}$	$\left(\frac{N^0_{max\|0}}{N^0_{max\|G}}\right)\frac{\rho a_h B}{C_0}$	$\left(\frac{N^0_{max\|0}}{N^0_{max\|G}}\right)\frac{\rho a_h r}{C_0}$
CONSTRAINTS				
$\bar{N}$	$0<\bar{N}\leq(1-m\bar{F}_h^{c_m})^{c_k}$			
$\bar{V}$	$\lvert\bar{V}\rvert\leq\frac{1}{\pi+2}$	$\lvert\bar{V}\rvert\leq\frac{1}{6.05}$	$\lvert\bar{V}\rvert\leq\frac{1}{\pi+2}$	$\lvert\bar{V}\rvert\leq\frac{1}{6.05}$

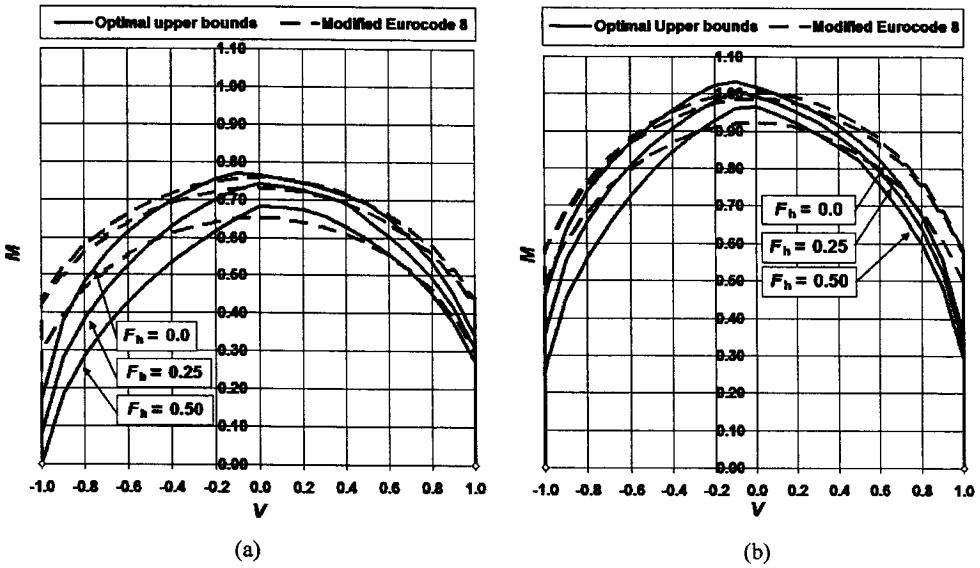

Fig. 20. Optimal upper bounds and modified Eurocode 8 results for heterogeneous soils. Interaction diagram ($N = 1/3\, N^0_{max}$ V, M, F_h) for circular footing on soil with no tensile strength: a) $k = 1$ and b) $k = 3$

results, although considered to be close to the exact ultimate loads, are upper bounds and they are thus found on the unsafe side of the design.

ACKNOWLEDGMENTS

The first author wishes to thank the Ecole Polytechnique (Laboratoire de Mécanique des Solides) and the Welfare Foundation "Alexandros S. Onassis" for the financial support during the execution of this study.

NOTATION

Greek small

β, γ = Constant parameters in the analytical expression of the EC8
$\underline{\gamma}$ = Soil unit weight
δ = Geometrical parameter in mechanisms
ε = Geometrical parameter in mechanisms
κ = Geometrical parameter in mechanisms
λ = Geometrical parameter in mechanisms
μ = Geometrical parameter in mechanisms
π = Function of maximum resisting work
ρ = Soil mass density
σ = Normal component of the stress vector on a plane
$\underline{\underline{\sigma}}$ = Stress tensor
T = Tangential component of the stress vector on a plane
$\underline{\hat{\omega}}$ = Virtual angular velocity

Greek capital

Σ = Velocity jump surface
Ω = Half-space of soil domain

Latin small

$\underline{a}$ = Earthquake-induced soil acceleration
a, b, c, d, e, f, m = constants parameters in the analytical expression of the EC8
c_N, c'_N, c_T, c_M, c'_M = constants parameters in the analytical expression of the EC8
$\underline{\underline{\hat{d}}}$ = *Virtual strain rate tensor*
f_{soil} = Strength criterion of soil medium
f_{interf} = Strength criterion of soil-foundation interface
k = Degree of heterogeneity
$\underline{n}$ = Unit normal vector
$\dot{q}_i$ = Associated kinematic parameter for Q_i
q = Surface load on the soil surface
r = Radius of the foundation
$\mathrm{tr}(\underline{\underline{\hat{d}}}) = \hat{d}_1 + \hat{d}_2 + \hat{d}_3$ = Trace of the strain rate tensor

Latin Capital

A = Foundation surface area
B = Width of a strip footing
F_h = Magnitude of horizontal inertial force in the soil
$\underline{F_h}$ = Vector of horizontal inertial force in the soil
M = Magnitude of moment on the footing
M_{Ed} = Moment for Earthquake design
$\underline{M}$ = Vector of moment on the footing
N = Magnitude of vertical force
N_{Ed} = Vertical force for Earthquake design
$\underline{N}$ = Vector of vertical force

N^0_{max} = Static bearing capacity under centered load
Q_i = Loading parameter of the system
$\hat{U}$ = Virtual velocity
$[\hat{U}]$ = Virtual velocity jump
V = Magnitude of horizontal force
V_{Ed} = Horizontal force for Earthquake design
$\underline{V}$ = Vector of horizontal force

REFERENCES

1) Bransby, M. F. and Randolph, M. F. (1998): Combined loading of skirted foundations, *Géotechnique*, **48**(5), 637–655.
2) Coleman, T. F. and Li, Y. (1996): An interior trust region approach for nonlinear minimization subject to boundso, *SIAM Journal on Optimization*, **6**(2), 418–445.
3) Cuvillier, A. (2001): *Aspects Mécaniques du Creusement d'un Tunnel en Milieu Poreux Saturé*, Thèse ENPC, Paris.
4) Dormieux, L. and Pecker, A. (1995): Seismic bearing capacity of foundation on cohesionless soil, *Journal of Geotechnical Engineering ASCE*, **121**(3), 300–303.
5) Eason, G. and Shield, R. T. (1960): The plastic indentation of a semi-infinite solid by a perfectly rough circular punch, *J. Appl. Math. Phys.* (ZAMP), **11**, 33 - 43.
6) EUROCODE 8 (1998): *Partie 5, Conception et Dimensionnement des Structures Pour Leur Résistance Aux Séismes*, Commission Européenne de Normalization. prENV 1998.
7) Fishman, K. L., Richards, R. and Yao, D. (2003): Inclination factors for seismic bearing capacity, *Journal of Geotechnical and Geoenvironmental Engineering ASCE*, **129**(9), 861–865.
8) Gouvernec and S., Randolph, M. (2003): Effect of strength nonhomogeneity on the shape of failure envelopes for combined loading of strip and circular foundations on clay, *Geotechnique*, **53**(6), 575–585.
9) Green, A. P. (1954): The plastic yielding of metal junctions due to combined shear and pressure, *Journal of Mechanics and Physics of Solids* **2**(3), 197–211.
10) Hansen Brinch, J. (1953): *Earth Pressure Calculation*, The Danish Technical Press–Institution of Danish Civil Engineers, Copenhagen.
11) Houlsby, G. T. and Martin, C. M. (1993): Modelling of the behaviour of foundations of jack-up units on clay, *Predictive Soil Mechanics*, Thomas Telford, London, 339–358.
12) Knappett, J. A., Haigh, S. K. and Madabhushi, S. P. G. (2006): Mechanisms of failure for shallow foundations under earthquake loading, *Soil Dynamics and Earthquake Engineering*, **26**(2–4), 91–102.
13) Kumar, J. and Mohan Rao, V. B. K. (2002): Seismic bearing capacity factors for spread foundations, *Géotechnique*, **52**(2), 79–88.
14) Mendoza, M. J. and Auvinet, G. (1988): The Mexico earthquake of September 19, 1985–Behavior of building foundations in Mexico City, *Earthquake Spectra*, **4**(4), 835–852.
15) Paolucci, R. and Pecker, A. (1997a): Soil inertia effects on the bearing capacity of rectangular foundations on cohesive soils, *Engineering Structures*, **19**(8), 637–643.
16) Paolucci, R. and Pecker, A. (1997b): Seismic bearing capacity of shallow strip foundations on dry soils, *Soils and Foundations*, **37**(3), 95–105.
17) Pecker, A. (1997): Analytical formulae for the seismic bearing capacity of shallow strip foundations, *Seismic Behavior of Ground and Geotechnical Structures* (ed. by Seco e Pinto), Balkema, 261–268.
18) Pecker, A. and Salençon, J. (1991): Seismic bearing capacity of shallow strip foundations on clay soils, *Proc. International Workshop on Seismology and Earthquake Engineering*, Mexico City, 22–26 April 1991, CENAPRED Mexico City, 287–304.
19) Puzrin, A. M. and Randolph, M. F. (2003a): Generalized framework for three-dimensional upper bound limit analysis in a Tresca material, ASME, *Journal of Applied Mechanics*, **70**(1), 91–100.
20) Puzrin, A. M. and Randolph, M. F. (2003b): New planar velocity fields for upper bound limit analysis, *International Journal of Solids and Structures*, **40**(13–14), 3603–3619.
21) Randolph, M. F., Cassidy, M., Gouvernec, S. and Erbrich, C. (2005): Challenges of offshore geotechnical engineering, *Proc. 16th ICSMFE*, 123–176.
22) Randolph, M. F. and Puzrin, A. M. (2003): Upper bound limit analysis of circular foundations on clay under general loading, *Geotechnique*, **53**(9), 785–796.
23) Richards, R. JR., Elms, D. G. and Budhu, M. (1993): Seismic bearing capacity and settlements of foundations, *Journal of Geotechnical Engineering*, ASCE, **119**(4), 662–674.
24) Salençcon, J. (1983): *Calcul à la Rupture et Analyse Limite*, Presses de l'E.N.P.C., Paris.
25) Salençon, J. (1990): An introduction to the yield design theory and its applications to soil mechanics, *European Journal of Mechanics, A/Solids*, **9**(5), 477–500.
26) Salençon, J. (2002): *de l'élastoplasticité au Calcul à la Rupture*, Éditions de l'École Polytechnique, Palaiseau.
27) Salençon, J. and Matar, M. (1982): Capacité portante des fondations superficielles circulaires, *Journal de Mécanique théorique et appliquée*, **1**(2), 237–267.
28) Salençon, J. and Pecker, A. (1995a): Ultimate bearing capacity of shallow foundations under inclined and eccentric loads. Part I: Purely Cohesive Soil, *European Journal of Mechanics, A/Solids*, **14**(3), 349–375.
29) Salençon, J. and Pecker, A. (1995b): Ultimate bearing capacity of shallow foundations under inclined and eccentric loads, Part II: Purely Cohesive soil without tensile strength, *European Journal of Mechanics, A/Solids*, **14**(3), 377–396.
30) Sarma, S. K. and Iossifelis, I. S. (1990): Seismic bearing capacity factors of shallow strip footings, *Géotechnique*, **40**, 265–273.
31) Sekiguchi, H. and Kobayashi, S. (1997): Limit analysis of bearing capacity for a circular footing subjected to eccentric loadings, *Proc. 14th ICSMFE*, Hamburg, Germany, 1997, **2**, 1029 - 1032.
32) Subrin, D. and Wong, H. (2002): Stabilite du front d'un tunnel en milieu frottant: un nouveau mécanisme de rupture 3D, *C. R. Mécanique*, **330**(7), 513–519.
33) Zeng, X. and Steedman, R. S. (1998): Bearing capacity failure of shallow foundations in earthquakes, *Géotechnique*, **48**(2), 235–256.